NJC

PAPER

View Article Online
View Journal | View Issue

Cite this: *New J. Chem.*, 2017, **41**, 316

Metal-mediated generation of triazapentadienate-terminated di- and trinuclear μ_2-pyrazolate Ni^{II} species and control of their nuclearity†

Elena V. Andrusenko, Evgeniy V. Kabin, Alexander S. Novikov, Nadezhda A. Bokach,* Galina L. Starova and Vadim Yu. Kukushkin*

Received (in Victoria, Australia) 20th September 2016,
Accepted 15th November 2016

DOI: 10.1039/c6nj02962k

www.rsc.org/njc

1,3,5-Triazapentadienate-terminated di- and trinuclear nickel(II) complexes featuring bridging azolate ligands, $[Ni_2(\mu_2\text{-azolate})_2(TAP)_2]$ (TAP = HN═C(OMe)NC(OMe)═NH; azole = 3,5-Me_2pyrazole **2**, 3,5-Ph_2pyrazole **3**) and $[Ni_3(\mu_2\text{-azolate})_4(TAP)_2]$ (azole = 3,5-Me_2pyrazole **4**, indazole **5**), were obtained from systems Ni^{2+}/$NCNR_2$/azole systems in MeOH. The terminal TAP ligands in the $[Ni_2(\mu_2\text{-azolate})_2(TAP)_2]$ and $[Ni_3(\mu_2\text{-azolate})_4(TAP)_2]$ species originate from the previously unreported cascade Ni^{II}-mediated and chelation-driven reaction between cyanamides and methanol. The oligomeric species and also $[Ni(TAP)_2]$ (**1**) are subject to interconversions that depend on the reactants involved and the reaction conditions. The control of the nuclearity of the complexes can be achieved by changing the amount of azoles or by their protonation, alteration of the steric hindrance of the substituents in the heterocycles, and by changing the reaction temperature. Complexes **1**–**4** were characterized using elemental (C, H, N) analyses, ^{1}H, ^{13}C{^{1}H} NMR, FTIR, HRESI-MS, TG-DTA, X-ray crystallography, and **5** was characterized using HRESI-MS and X-ray crystallography. Unconventional metallophilic contacts $Ni^{II}\cdots Ni^{II}$ were observed in dimer **3** in the solid state (the distance for Ni···Ni is 2.99 Å, whereas the double Bondi's vdW radius for Ni is 3.26 Å) and the reality of these interactions was confirmed theoretically by the topological analysis of the electron density distribution (AIM method). The estimated energy for these non-covalent Ni···Ni interactions (*ca.* 4 kcal mol^{-1}) fills the gap in the reported energies of the metal···metal interactions in a series comprising of $Ni^{II}\cdots Ni^{II}$ (this work), $Pd^{II}\cdots Pd^{II}$ (4.3–6.0 kcal mol^{-1}), and $Pt^{II}\cdots Pt^{II}$ (3.9–11.7 kcal mol^{-1}).

Introduction

The abundance of pyrazole(ate)-based ligands is due to the ability of these species to bind metals in a variety of coordination modes, in particular, as bridging ligands. In addition, pyrazole(ate) fragments can be integrated into metal species as they are or as a functionality of more complex polydentate ligands, *e.g.* polypyrazolylborates.[1] Metal complexes bearing pyrazole(ates) of different types found applications as catalysts,[2] magnetic,[2–3] luminescent,[2,4] gas storage or separation[2,4a,d] materials, useful compounds for medicine[2] and biomimetic chemistry,[5] and also as precursors for CVD.[4b] Several excellent reviews provide a general picture of the syntheses and application of pyrazole(ate) metal species.[2,3,4a,b,5]

When pyrazolates act as bridging ligands, they are capable of forming metal complexes exhibiting different nuclearity.[4a,6] In particular, nickel(II) centers react with unsubstituted pyrazole (HPz) giving the 1D-chain polymers, $[Ni(Pz)_2]_n$ (Fig. 1, type **A**), as two thermochromic[7] crystalline phases.[7–8] Nickel(II) complexes featuring bis-pyrazolate ligands form porous MOFs possessing high thermal robustness and exhibiting adsorptive properties[9] and, in particular, MOFs based upon Ni(bpb) (H_2bpb = 1,4-(4-bispyrazolyl)benzene) act as a moisture resistant adsorbent toward thiophene.[9a] Nickel(II) and 3(5)-arylpyrazoles ($H^{Ar}Pz$) form binary cyclic trinuclear complexes $[Ni_3(^{Ar}Pz)_6]$ (type **B**).[10]

Examples of oligomeric species incorporating the $\{Ni(\mu\text{-}^{R}Pz)_2Ni\}$ fragment supported by other ligands include the dinuclear $[Ni_2Cp_2(^{RRR'}Pz)_2]$ (L = 1/2Cp, type **C**) and the trinuclear $[Ni_3Cp_2(^{RRR'}Pz)_4]$ (L = 1/2Cp, type **D**) species that were obtained from the 3,4,5-substituted pyrazoles $H^{RRR'}Pz$ and Cp_2Ni.[11] The nuclearity of these complexes depends on the bulkiness of the 3- and 5-substituents in the pyrazolate moiety[11a] and also on the reaction temperature.[11b] It is reported that the sterically hindered substituents and low synthesis temperature favor dimetallic rather than trimetallic species. It is noteworthy that

Institute of Chemistry, Saint Petersburg State University, Universitetskaya Nab. 7/9, 199034, Saint Petersburg, Russian Federation. E-mail: n.bokach@spbu.ru, v.kukushkin@spbu.ru

† Electronic supplementary information (ESI) available: CCDC 1440113, 1440114, 1440621, 1442880, and 1453872. For ESI and crystallographic data in CIF or other electronic formats see DOI: 10.1039/c6nj02962k

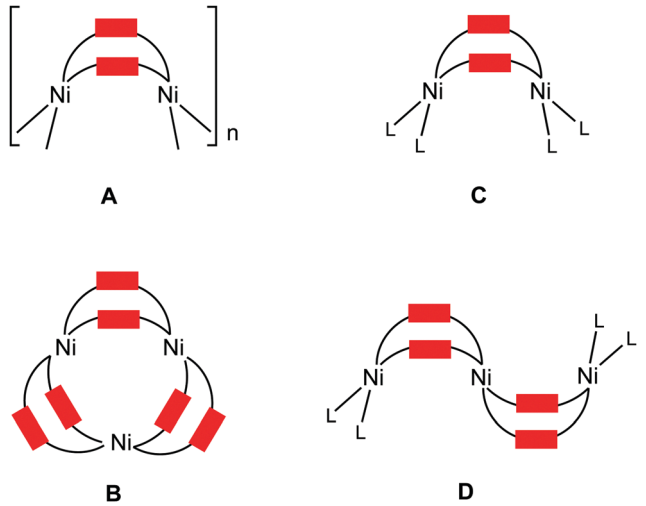

Fig. 1 Selected types of nickel(II) complexes featuring the {Ni(μ-^{R}Pz)$_2$Ni} moiety.

before our current work, interconversion of di- and trinuclear species (see later) had never been studied.[11]

The homodinuclear complexes of the type [Ni$_2$($^{RRR'}$Pz)$_2$L$_4$] (RRR′ = Me$_3$, L = 1/2 bis(imidazolyl)(pyrazolyl)borate;[12] R = Me, R′ = H, L = 1/2 3,5-dimethylpyrazole-1-carbodithioate;[13] R = H, R′ = Me, or R = R′ = H, L = C_6F_5;[14] $^{RRR'}$PzL$_2$ = 3,5-bis((1-(2,6-diisopropylphenyl)-1*H*-imidazol-3-ium-3-yl)methyl)pyrazol-1-ate;[15] $^{RRR'}$PzL$_2$ = 3,5-bis((1-methyl-1*H*-imidazol-3-ium-3-yl)methyl)pyrazol-1-ide;[16] type **C**) were also reported. Two dinuclear NHC/pyrazolate complexes [Ni$_2$L](PF$_6$)$_2$ (type **C**) bearing the macrocyclic ligand were generated from [H$_6$L](PF$_6$)$_4$ ([H$_6$L]$^{4+}$ = methylene- and ethylene-bridged calix[4]imidazolium[2]-pyrazole cyclophane),[17] and the latter complex is able to selectively recognize halides and self-assemble with guest anions (Cl$^-$ and Br$^-$).[17b] The {Ni(μ-PzR)$_2$Ni} motif was identified in the highly porous and robust [Ni$_8$(OH)$_4$(OH$_2$)$_2$(4,40-(buta-1,3-diyne-1,4-diyl)bispyrazolate)$_6$]$_n$ MOF,[18] in the octanuclear [Ni$_8$(μ$_4$-O)$_6$(Pz)$_{12}$]$^{2-}$ complex possessing a cube structure,[3e] and in a Ni$_9$ cluster-bearing bridged μ$_2$-pyrazolate, μ$_6$-CO_3^{2-}, and μ$_3$-OH$^-$ ligands which display cluster glass-like magnetic behavior.[19] The indazole (IndH) analog featuring the {Ni(μ-Ind)$_2$Ni} group was only observed for the [Ni$_2$(μ-Ind)$_2$(C$_6$F$_5$)$_4$]$^{2-}$ complex.[14]

In view of our general interest in ligand reactivity and, in particular, in metal-mediated and metal-catalyzed transformations of conventional nitriles and cyanamides[20] with pyrazolate-based systems,[21] we extended our project to reactions of (azole)Ni^{II} (azole = pyrazole, indazole) species with NCNR$_2$. Taking into account that (azolate)$_2$Ni^{II} complexes may have some applied significance, for instance in anion recognition chemistry (see, *e.g.*, ref. 17*b*), we planned to understand how to control the nuclearity of nickel(II)–azole systems in order to obtain a rational approach for the generation of well-defined (azolate)$_2$Ni^{II} species. Our goals were to develop a rational route to oligomeric Ni^{II} complexes featuring the {Ni(μ$_2$-azolate)$_2$}$_n$ fragment and to study how the nuclearity and structure of these Ni^{II}-based pyrazolate oligomers depend on reaction conditions and the nature of the reactants.

Results and discussion

To study the Ni^{II}-involving reactions between cyanamides and azole-type heterocycles we chose nickel salts NiX$_2$·*n*H$_2$O (X = Cl, OTf, *n* = 0; Br, *n* = 3; I, *n* = 6), *N*,*N*-disubstituted cyanamides NCNR$_2$ (R$_2$ = Me$_2$, Et$_2$, C$_5$H$_{10}$, C$_2$H$_4$OC$_2$H$_4$), and also pyrazoles and indazole as depicted in Fig. 2.

We studied the reaction of dialkylcyanamides with the azoles in the presence of nickel(II) salts in methanol, where the nickel salts are well soluble. In these reactions, di- and trinuclear nickel(II) complexes bearing bridging μ$_2$-azolate and terminal 1,3,5-triazapentadienate (abbreviated as TAP) ligands were obtained as major products. We observed (see later) that the TAP ligand originates from an unusual cascade of Ni^{II}-mediated and chelation-driven cyanamide–methanol integration, and that TAP generation is not affected by the presence of any one of the azoles. Methanol in the reaction serves as both a reagent and a solvent and in view of that we decided to study the Ni^{II}-mediated reaction of dialkylcyanamides with different alcohols, whereupon we included the azoles in the tested systems. Our results are sequentially disclosed in the sections that follow.

Nickel(II)-mediated and chelation-driven cascade reaction of NCNR$_2$ and MeOH

The Ni^{II}-mediated integration between cyanamides and alcohols was conducted in alcohols R′OH (R′ = Me, Et, ^{i}Pr). The reactions of NiX$_2$·*n*H$_2$O and NCNR$_2$ (Scheme 1) were attempted at molar ratios in the range between 1 : 2 and 1 : 10 and all tests were conducted either at RT or at 50 °C (for a detailed discussion of the reaction conditions see the ESI†).

We observed that the cascade generation of (TAP)Ni^{II} from NCNR$_2$ proceeds in MeOH after maintaining the reaction mixture for two weeks at RT or for 3 d at 50 °C and this reaction gives the complex [Ni(TAP)$_2$] (**1**; TAP = HN=C(OMe)NC(OMe)=NH; Scheme 1, a). Compound **1** was isolated as orange crystals after complete evaporation of the solvent and separation of the residue *via* column chromatography (yields up to 40%; for detailed characterization of **1** see the ESI†).

Bis-chelated complex **1** can be formed in a Ni^{II}-mediated and chelation-driven cascade reaction of dimethylcyanamide with

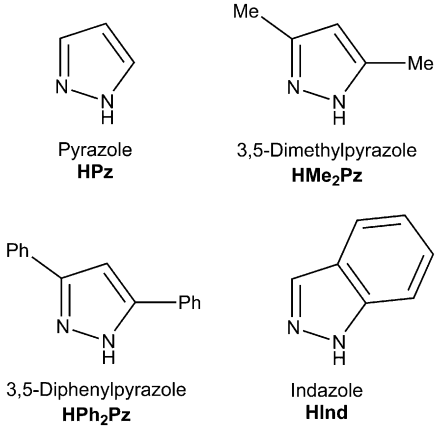

Fig. 2 The azoles applied in this study, their IUPAC names, and abbreviations.

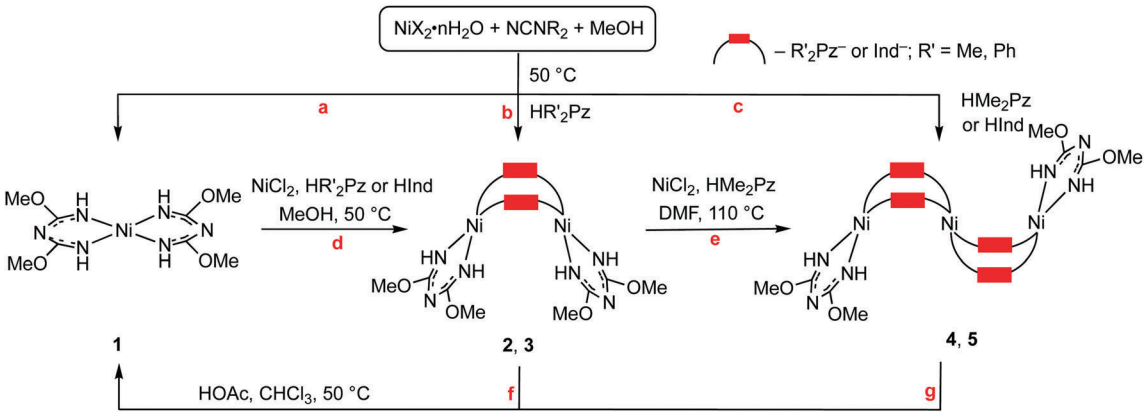

Scheme 1 Reaction between the azoles, cyanamides, and nickel salts in methanol.

MeOH. Moreover, MeOH plays the role of an alkylation reagent supporting NR_2/OMe replacement in the formed species, and other products derived from the methylation of the NR_2 group, *viz.* $[Me_2NR_2]X$ were identified using $HRESI^+$-MS (for a detailed discussion of the postulated reaction mechanism see the ESI†).

Complexes of the type M{HN═C(OR)NC(OR)═NH} have been reported for late transition metals, *e.g.* Co^{III},[22] Ni^{II},[22b] Cu^{II},[22,23] Zn^{II},[22b,23a,b,24] and Pd^{II}.[25] These chelates were obtained either through a chelation-driven reaction of the dicyanimides, $(NC)_2NNa$ or $(NC)_2NH$, with alcohols in the presence of a transition metal salt (Cu^{II},[14] Zn^{II}[10,12]) or *via* the transmetalation of $[M\{HN{=}C(OR)NC(OR){=}NH\}_2]$ (M = Cu^{II} or Zn^{II}) with other metal centers such as, for instance, Co^{III}.[22a,23a,b]

Nickel(II)-mediated reaction of $NCNR_2$ with the azoles in alcohols

Mixing $NiX_2{\cdot}nH_2O$ (X = Cl, OTf, n = 0; Br, n = 3; I, n = 6) with $NCNR_2$ (R = Me_2, Et_2, C_5H_{10}, $C_2H_4OC_2H_4$) and the azoles in methanol at RT or 50 °C (see the more detailed discussion later) results in the generation of the di- and trimeric complexes $[Ni_2(\mu_2\text{-}R'_2Pz)_2(TAP)_2]$ (R′ = Me **2**, Ph **3**) and $[Ni_3(\mu_2\text{-}Me_2Pz)_4(TAP)_2]$ (**4**) (Scheme 1, b and c). The reactions were performed in all possible combinations of the reactants and molar ratios between $NiX_2{\cdot}nH_2O$ and $NCNR_2$ that range from 1 : 2 to 1 : 6 and between $NCNR_2$ and the azoles that are in the interval from 1 : 0.5 to 1 : 4 and two temperatures, *i.e.* RT and 50 °C.

Although all four cyanamides underwent the reaction, two of them (R_2 = Me_2, $C_2H_4OC_2H_4$) demonstrated greater reactivity and gave higher yields of **2–4**; these two cyanamides were also the most efficient in the generation of the TAP ligand (see previous section). The di- and trinuclear complexes were obtained for the substituted pyrazoles, *i.e.* HMe_2Pz and HPh_2Pz. Among the tested nickel salts, the highest yields of **2–4** were obtained with NiX_2 (X = Cl, OTf). Concurrently, the reaction with the unsubstituted pyrazole (R′ = H) after 10 min (MeOH, either RT or 50 °C) gave the previously reported crystalline polymeric α-$[Ni(Pz)_2]_n$ (for its identification by powder XRD see Fig. S25, ESI†),[8] which is poorly soluble in all commonly used solvents.

For the systems NiX_2/$NCNR_2$/azole (X = Cl, OTf; R_2 = Me_2), the composition of the product depends on the temperature, anion X, and substituent R′ in the heterocycle. For HMe_2Pz and $NiCl_2$ at 50 °C, only trimer **4** was isolated (43%), while at RT both **2** and **4** species were obtained. Pure dimer **2** was obtained when excess of $NCNR_2$ was applied in the reaction with $NiCl_2$ ($NiCl_2$: $NCNR_2$ ratio was 1 : 4 or 1 : 6) at RT and when $Ni(OTf)_2$ reacted with HMe_2Pz and $NCNR_2$ at either RT, or at 50 °C (yield up to 25%). The HPh_2Pz forms dimer **3** in all tested combinations of $NCNR_2$ and NiX_2 and the highest yield of **3** (34%) was obtained for the system $NiCl_2$/$NCNMe_2$/HPh_2Pz (molar ratio 1 : 4 : 2). In other cases, the obtained optimal molar ratios between $NCNR_2$ and the azoles were 4 : 2 (**2**) and 1 : 4 (**4**) at a 0.1 M concentration of NiX_2 (1 equiv.).

The reaction that involves the unsymmetrical indazole and $NCNR_2$ should potentially give a mixture of regiosiomeric species. Indeed, we observed using both NMR and HRESI-MS the generation of a broad spectrum of products that we failed to separate using column chromatography due to similar retention or to isolate the products in the pure form *via* fractional crystallization. A few single-crystals of $[Ni_3(\mu_2\text{-Ind})_4(TAP)_2]$ (**5**) were mechanically picked out from the $NiCl_2$/$NCNMe_2$/HInd (1 : 1 : 4, 5 d, 50 °C) reaction mixture and were characterized by XRD (see later). The solid residue obtained after evaporation of the solvent contains a mixture of **5** with other yet unidentified products. The $HRESI^+$-MS of this residue displays several groups of peaks corresponding to $[HN{=}C(OMe \text{ or } NMe_2)NHC(NMe_2){=}NH_2]^+$, $[Ni(C_2H_2N_3)_2(OMe)_x(NMe_2)_{4-x} + H]^+$ (x = 1–4), $[Ni_2(\mu_2\text{-Ind})_2\text{-}(C_2H_2N_3)_2(OMe)_x(NMe_2)_{4-x} + H]^+$ (x = 1–3), and $[Ni_3(\mu_2\text{-Ind})_4\text{-}(C_2H_2N_3)_2(OMe)_x(NMe_2)_{4-x} + H]^+$ (x = 1–3) (ESI,† Fig. S8).

X-ray crystallographic studies for 2–5

Single-crystal XRD studies were performed for **2–5** (Fig. 3–6). The structure of **3** is built up of two crystallographically independent molecular units, whereas all other structures consist of one molecular unit. In the structures of the dimers and trimers, the nickel atoms exhibit square-planar environments formed with four N atoms from the TAP ligand or a substituted azolate (see more information regarding the X-ray crystallographic studies in the ESI†).

Consideration of the crystallographic data suggests the presence of Ni···Ni metallophilic interactions in the di- and

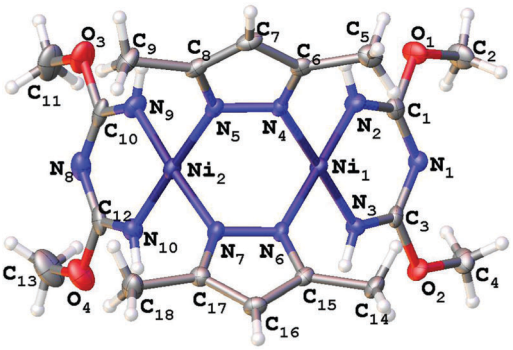

Fig. 3 Molecular structure of **2** with the atomic numbering scheme. Thermal ellipsoids are given at the 50% probability level.

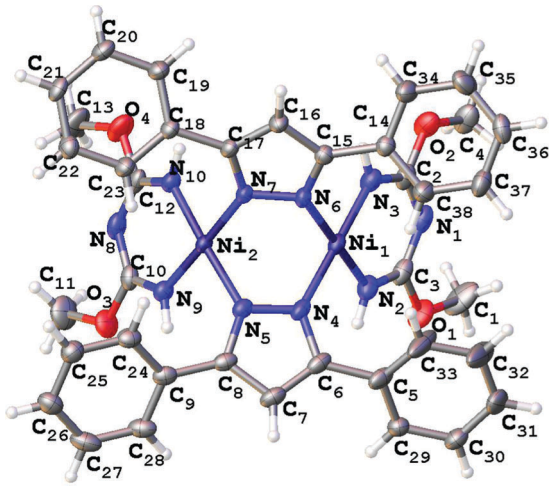

Fig. 4 Molecular structure of **3** with the atomic numbering scheme. Thermal ellipsoids are given at the 50% probability level.

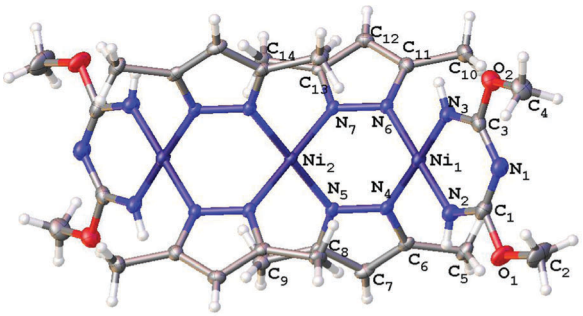

Fig. 5 Molecular structure of **4** with the atomic numbering scheme. Thermal ellipsoids are given at the 50% probability level.

trinuclear structures. Indeed, inspection of the XRD data reveals that the interatomic distances between the Ni atoms in **2** (3.10 Å), **3** (2.99 Å), and **4** (3.25 Å) are less than the sum of their Bondi's (the shortest) van der Waals radii[26] (3.26 Å for Ni + Ni atoms). In order to confirm or deny the assumption on the presence of Ni···Ni metallophilic interactions in **2**–**4** and to quantitatively estimate their energies we carried out theoretical DFT calculations and performed topological analysis of the

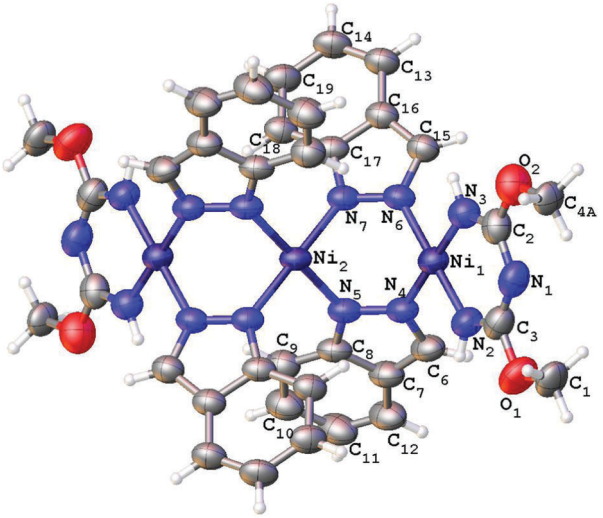

Fig. 6 Molecular structure of **5** with the atomic numbering scheme. Thermal ellipsoids are given at the 50% probability level.

electron density distribution within the formalism of Bader's theory (AIM method; for more detailed information see the ESI†).[27] This approach has already been successfully used by us to study the non-covalent interactions and properties of the coordination bonds in transition metal complexes.[28]

Theoretical consideration of Ni···Ni metallophilic interactions in 3

Metallophilic interactions impart important properties to functional materials such as luminescence,[29] polychromism,[30] magnetism,[31] or one-dimensional electrical conductivity.[32] This phenomenon is generally considered as weak attractive interactions between adjacent metal centers due to overlapping of their d_z^2 and p_z orbitals[33] and it has been intensively studied in recent years. Most reports in this area are related to the solid state, where structural parameters obtained by XRD provide precise information on metal···metal separations.

The strength of such M···M interactions is comparable to weak or medium hydrogen bonding, *e.g.*, for Au···Au aurophilic interactions (the strongest one) the appropriate bond energy is *ca.* 7–12 kcal mol^{-1},[34] whereas other metallophilic interactions are usually weaker because the influence of relativistic effects in such cases is lower, and the ability of atoms to be involved in this type of bonding increases down through the group. The $M^I \cdots M^I$ (M = Cu, Ag, Au) metallophilic interactions are certainly most studied.[35] For group 10 elements, metallophilic interactions of heavy elements (*i.e.* $Pt^{II} \cdots Pt^{II}$ (ref. 36) and $Pd^{II} \cdots Pd^{II}$(ref. 37)) are quite common, whereas $Ni^{II} \cdots Ni^{II}$ short contacts were detected for a significantly lower number of systems.[12,38] Their metallophilic nature was never confirmed using theoretical studies and, consequently, their energies were not estimated.

The AIM analysis (ESI,† Fig. S7) did not reveal Ni···Ni interactions in **2** and **4**. However, in **3**, exhibiting the shortest Ni···Ni distance, we succeeded to find an appropriate bond critical point (3, −1) (BCP) (Fig. 7). The low magnitude of the

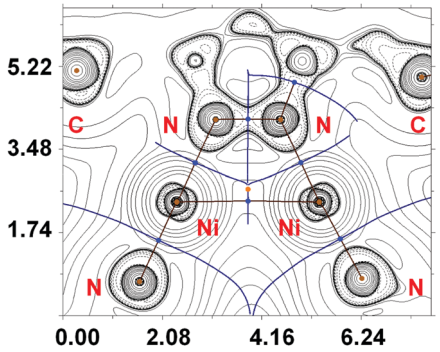

Fig. 7 Contour line diagrams of the Laplacian distribution $\nabla^2\rho(r)$, bond paths and selected zero-flux surfaces for **3**. Bond critical points (3, −1) are shown in blue, nuclear critical points (3, −3) in pale brown and ring critical points (3, +1) in orange; the length unit is Å.

electron density (0.016–0.017 Hartree), positive values of the Laplacian (0.046–0.052 Hartree), and close to zero energy density (−0.001) in this BCP are typical for non-covalent interactions. We have defined energies (3.5–4.4 kcal mol^{-1}) for this contact according to the procedures proposed by Espinosa *et al.*[39] and Vener *et al.*[40] The covalent contribution in the Ni···Ni metallophilic interactions in **3** is negligible (for details see the ESI†). It is noteworthy that the estimate of the properties of electron density in BCP and energies for the metallophilic interactions Ni···Ni in **3** weakly depends on the basis set used (relativistic or non-relativistic approaches).

Although the analysis of the XRD data for **2–4** indicates that in all three cases Ni···Ni separations are less that the double Bondi's van der Waals radius for Ni, the conducted DFT calculations allowed the reliable identification of these metallophilic contacts only in one case (complex **3** with the shortest Ni···Ni distance). Even for **3**, the theoretically determined energies of the nickel(II)···nickel(II) interactions are rather low and certainly lower than those found for the Pd^{II}···Pd^{II} (4.3–6.0 kcal mol^{-1}, ref. 37) and Pt^{II}···Pt^{II} (3.9–11.7 kcal mol^{-1}, ref. 36*a–g*) systems. Taking all these into account, we believe that the emergence of nickel(II)···nickel(II) interaction in **3** is, at least partially, determined by crystal packing effects.

Interconversions of 1–4

We found that di- and trinuclear complexes **2–4** could be converted to monomeric **1**. In contrast, **1** could give **2–4** when reacting with the appropriate azole and $NiCl_2$. Thus, complexes **2** and **4** in a chloroform solution transform to **1** by acidification with 1 equiv. HOAc and by keeping the mixture at 50 °C for 2 d (yields of **1** are 19 and 22%, respectively; Scheme 1, f and g); formation of **1** was confirmed using HRESI-MS and single-crystal XRD. Acidification of a solution of **4** gives solely **1** with no traces of **2**.

Heating of a mixture of **1** and $NiCl_2$ (a molar ratio of 1 : 1; MeOH solution) with HR'_2Pz (R′ = Me, Ph; 8 equiv.) for 1 d at 50 °C leads to the gradual release of yellow crystals of **2** or **3** (yields 19 and 14%, respectively; Scheme 1, d). The formation of **2** and **3** was confirmed using HRESI-MS and by both powder and single-crystal XRD. HRESI-MS analysis of the mother liquor demonstrates the presence of unreacted **1** and some intermediate products, *e.g.* the cationic $[Ni(Ph_2Pz)_2(TAP)]^+$ species. The HRESI$^+$-MS spectra of the reaction mixture comprising of **1**, $NiCl_2$, and IndH (a molar ratio of 1 : 1 : 8; 7 d, 50 °C, MeOH) exhibit several groups of peaks corresponding to the $[TAP + 2H]^+$, $[Ni(TAP)_2 + H]^+$, $[Ni_2(\mu_2\text{-Ind})_2(TAP)_2 + H]^+$, and $[Ni_3(\mu_2\text{-Ind})_4(TAP)_2 + H]^+$ ions (Fig. S16, ESI†). Therefore, although the formation of indazolate-based oligomers takes place under the reaction conditions, all our attempts to isolate individual products were, unfortunately, unsuccessful.

Dimer **2** was converted to trimer **4** when a mixture of **2** and $NiCl_2$ (in a molar ratio of 1 : 1) was heated with 3 equiv. $NCNMe_2$ and excess HMe_2Pz at 110 °C in DMF for 1 d (yield 52%; Scheme 1, e). Formation of **4** was confirmed using HRESI$^+$-MS and powder XRD, while HRESI$^+$-MS analysis of the mother liquor demonstrates the presence of unreacted **2**.

These interconversions of **1–4** explain the relatively low yields of **2–4** and the strong dependence of the outcome of the reaction on the molar ratio of the reactants. Analysis of the reaction mixtures using HRESI-MS indicates the co-existence of several mono-, di-, and trimeric (azolate)$_2$Ni^{II}-based species, while their corresponding tetramers and nickel-containing species of higher nuclearities were not detected even upon prolonged heating of the resection mixtures at 50 °C in DMF or at 140–160 °C in $HOCH_2CH_2OH$.

Conclusions

The results of this work can be considered from the following main perspectives. We synthesized two triazapentadienate-terminated di- and two trinuclear Ni^{II} complexes featuring the bridging azolate ligands, $[Ni_2(\mu_2\text{-azolate})_2(TAP)_2]$ and $[Ni_3(\mu_2\text{-azolate})_4(TAP)_2]$ (TAP = HN=C(OMe)NC(OMe)=NH). We observed that these dimers and trimers and also $[Ni(TAP)_2]$ could undergo interconversions depending on the reactants involved and the reaction conditions (Scheme 1).

The nuclearity of the complexes depends on the amount of azoles (or, in contrast, acid) in the system, steric hindrance of the substituents in the ring systems, and the temperature of the reaction. A higher amount of azoles leads to higher nuclearity systems, whereas the addition of an acid promotes conversion of trimers to dimers and then to $[Ni(TAP)_2]$. As it is more sterically demanding, due to the restricted rotational freedom in the complexes, H(3,5-Ph$_2$)Pz forms only dimer **3**, whereas H(3,5-Me$_2$)Pz gives dimeric **2** and trimeric **4** species. Higher temperature favors the generation of trimeric **4** rather than dimeric **2**.

All these observations open up a route to control both the nuclearity of nickel(II)–azole complexes and allows the synthesis of well-defined (azolate)$_2$Ni^{II} species. Partially our observations are in agreement with those reported previously for azolate species bearing the terminal CpNi fragment.[11] Although in these two studies the dependence of nuclearity on the amount of azole/acid was not established, the authors observed the dependence of the nuclearity of (azole)Ni^{II} species on both the steric hindrance of azoles and temperature. We expect that our

data might be useful in the generation of nickel(II) systems of higher nuclearity in, *e.g.* solvothermal syntheses.[41]

Using XRD we detected unconventional nickel(II)···nickel(II) metallophilic interactions in **3**, and provided the first case where the availability of these metallophilic interactions was confirmed theoretically using a DFT method. Furthermore, we succeeded in getting an estimate of the energy for these non-covalent contacts (3.5–4.4 kcal mol^{-1})—that is lower than those for $Pd^{II}\cdots Pd^{II}$ (4.3–6.0 kcal mol^{-1}, ref. 37) and $Pt^{II}\cdots Pt^{II}$ (3.9–11.7 kcal mol^{-1}, ref. 36*a–g*) systems—and it is believed that the existence of these $Ni^{II}\cdots Ni^{II}$ interactions is mainly determined by the packing effects. It has now been proven that the strength of the metallophilic interactions for compounds of group 10 elements increases down through the group according to their ability to overlap d_z^2 and p_z orbitals of the neighboring metal centers.

Experimental

Materials and instrumentation

Solvents, dialkylcyanamides, and nickel(II) salts $NiBr_2{\cdot}3H_2O$, $NiI_2{\cdot}6H_2O$, and $Ni(OTf)_2$ were obtained from commercial sources and used as received. Anhydrous nickel chloride was prepared according to a previously reported procedure.[42] FTIR spectra (4000–400 cm^{-1}) were recorded on a Shimadzu IR Prestige-21 instrument in KBr pellets (Fig. S9–S12 of the ESI†). Microanalyses (C, H, N) were carried out on a Euro EA3028-HT instrument. A standard EDTA method was utilized for Ni analysis of complex **1**.[43] Electrospray ionization mass-spectra were obtained on a Bruker micrOTOF spectrometer equipped with an electrospray ionization (ESI) source. The instrument was operated both in positive and negative ion modes in the *m*/*z* range 50–3000. For ESI, the complexes were dissolved in MeOH. In the isotopic pattern, the most intensive peak is reported (Fig. S8 and S13–S17, ESI†). GC-MS identification of the by-products from the synthesis of **1** was performed on a Shimadzu GCMS-QP2010 Ultra instrument equipped with a Stabilwax 30 m × 0.32 × 0.50 μm column. The temperature program was set at 70–230 °C with a linear rate of 10 °C min^{-1} and the column was held at 230 °C for 75 min. ^1H and $^{13}C\{^1H\}$ NMR (400.13 and 100.613 MHz, respectively) spectra were measured on a Bruker Avance 400 spectrometer in Me_2SO-d_6 (for **1**) and $CDCl_3$ (for **2–4**) at ambient temperature; residual solvent signals were used as the internal standard (Fig. S17–S24, ESI†). The TG-DTA study (Fig. S28–S31, ESI†) was performed using a NETZSCH TG 209 F1 Libra thermoanalyzer and MnO_2 powder was used as a standard. The initial weights of the samples were in the range of 0.9–1.4 mg. The experiments were run in an open aluminum crucible in a stream of argon at a heating rate of 10 K min^{-1}. The final temperature was 610 °C. Processing of the thermal data was performed using Proteus analysis software.[44] TLC was performed on Merck Silica gel 60G F_{254} plates.

X-ray crystal structure determination

For single-crystal XRD experiments all crystals were fixed on a micro mount and placed on an Agilent Technologies SuperNova diffractometer using CuK_α monochromated radiation (**1**, **3**, **5**) and on a Xcalibur, Eos diffractometer using MoK_α monochromated radiation (**2**, **4**); the crystals were measured at a temperature of 100 K. The structures were solved using the direct methods on a ShelXS[45] structure solution program (**2**, **3**) and Superflip[46] structure solution program (**1** and **4**). All structures were refined by means of the SHELX program[45] incorporated into the OLEX2 program package.[47] The crystallographic data and some refinement parameters are given in Table S3 (ESI†). The carbon-bound and nitrogen-bound H atoms were placed in the calculated positions and were included in the refinement in the 'riding' model approximation, with $U_{iso}(H)$ set to $1.5U_{eq}(C)$ and C–H 0.96 Å for the CH_3 groups, with $U_{iso}(H)$ set to $1.2U_{eq}(C)$ and C–H 0.93 Å for the CH groups, and with $U_{iso}(H)$ set to $1.2U_{eq}(N)$ and N–H 0.86 Å for the NH groups. Empirical absorption correction was applied in the CrysAlisPro program complex[21*b*] using spherical harmonics, implemented in the SCALE3 ABSPACK scaling algorithm. The unit cell of **3** also contains disordered molecules of the solvent that have been treated as a diffuse contribution to the overall scattering without specific atom positions using SQUEEZE/PLATON.[48] Crystallographic data for this paper were deposited at the Cambridge Crystallographic Data Centre and the CCDC numbers are 1440113, 1440114, 1440621, 1442880, and 1453875. Polycrystalline samples were studied in the 2θ range of 5–45° with a Bruker "D2 Phaser" powder diffractomer equipped with CuK_α source monochromated radiation.

Computational details

The single point calculations for **2–4** have been carried out at the DFT level of theory using the M06 functional (this functional describes reasonably weak dispersion forces and non-covalent interactions)[49] with the help of the Gaussian-09 program package.[50] The experimental X-ray geometries were taken as starting points. Two approaches were used in the present work, *viz.* (i) the Douglas–Kroll–Hess 2^{nd} order scalar relativistic calculations[51] requested relativistic core Hamiltonian were carried out using the DZP-DKH basis sets[52] for all atoms; (ii) the non-relativistic calculations were carried out using the standard 6-311+G* basis sets for all atoms. The topological analysis of the electron density distribution with the help of the atoms in molecules (AIM) method developed by Bader has been performed by using the Multiwfn program (version 3.3.4).[53] The Cartesian atomic coordinates for **2–4** are given in Table S2 (ESI†).

Syntheses and characterization

Generation of $[Ni(TAP)_2]$ (1). Any one of the nickel(II) salts $NiX_2{\cdot}nH_2O$ (X = Cl, OTf, *n* = 0; Br, *n* = 3; I, *n* = 6; 0.5 mmol) was dissolved in MeOH (3 mL), and $NCNR_2$ ($R_2 = Me_2$ or $C_2H_4OC_2H_4$; 2 mmol) was added to the solution. The green homogeneous reaction mixture was left to stand in air at RT for 2 weeks (or at 50 °C for 3 d) in a closed flask. The color of the reaction mixture gradually turned to bright-orange (X = Br, I) and a light-green precipitate was formed. In the case of X = Cl, the reaction mixture remained homogenous. The colorless crystals of $[Me_4N]X$ (X = Cl, Br, I) and/or $[Me_2NC_4H_8O]X$ (X = Cl, Br, I) were

precipitated from the reaction mixtures obtained at 50 °C. The reaction mixture (X = Cl; RT) or mother liquor, separated *via* filtration from the residue, was left to stand to undergo slow evaporation in air and orange crystals were formed after the complete evaporation of the solvent (2 d, RT). The crystalline product was dissolved in diethyl ether (3 mL) and the obtained solution was passed through a column filled with Merck silica gel 60 (0.063–0.200) (eluent EtOAc : hexane, 10 : 1, v/v). The red fraction was collected and evaporated to dryness at RT in air giving a crystalline product, which was dried over $CaCl_2$ in a desiccator at 20–25 °C.

[Ni(TAP)$_2$] (1). 57 mg, 35% (at RT), 63 mg, 39% (at 50 °C). R_f = 0.60 (acetone : hexane, 10 : 1, v/v). The complex sublimes at 175 °C upon heating. Calcd. for $C_8H_{16}N_6NiO_4$: C, 30.13; N, 26.35; H, 5.06; Ni, 18.40; Found: C, 30.19; N, 26.29; H, 5.04; Ni, 17.98. HRESI$^+$-MS, *m*/*z*: 319.0670 ([M + H]$^+$, requires 319.0670). ν_{max}(KBr)/cm^{-1}: 3364 m, 3344 m ν(N–H); 2994 s, 2950 s ν(C–H), 1614 *vs.* ν(C═N), 1394 s ν(C–O from OCH_3), 1214 s ν(C–N). ^{1}H NMR (DMSO-d_6): 3.58 (s, 3H, OMe), 4.66 (br s, 1H, NH). ^{13}C{^{1}H} NMR (DMSO-d_6): 54.0 (OCH_3), 163.1 (C═N). Crystals of **1** suitable for XRD were obtained by the slow evaporation of the reaction mixture at RT.

Ni^{II}-mediated reaction of cyanamides with the azoles in methanol

Syntheses of 2–4. $NiCl_2$ (6.4 mg, 0.5 mmol) was dissolved in MeOH (5 mL), and $NCNR_2$ (R_2 = Me_2, $C_2H_4OC_2H_4$; 2 mmol) and then HMe_2Pz (96 mg, 1 mmol) was added to the solution. The blue homogeneous reaction mixture formed was left to stand at 50 °C for 5 d in a closed flask. The color of the reaction mixture gradually turned to orange. The orange precipitate formed was decanted, washed with three 1.5 mL portions of MeOH and with three 1.5 mL portions of Et_2O. The crystalline product dried over $CaCl_2$ in a desiccator at 20–25 °C.

Complexes **3** and **4** were prepared similarly to **2**. $NiCl_2$ (64 mg, 0.5 mmol), MeOH (3 mL), $NCNR_2$ (R_2 = Me_2 or $C_2H_4OC_2H_4$; 2 mmol), and HPh_2Pz (220 mg, 1 mmol; for generation of **3**) or HMe_2Pz (192 mg, 2 mmol; for generation of **4**) were used. The reaction occurred for 4 (**3**) and 5 (**4**) days.

[Ni$_2$(μ$_2$-Me$_2$Pz)$_2$(TAP)$_2$] (2). 13.7 mg, 25%. Mp: 245 °C (dec.). Anal. calcd for $C_{18}H_{30}N_{10}Ni_2O_4$: C, 38.07; H, 5.32; N, 24.66. Found: C, 37.94; H, 5.33; N, 23.96%. HRESI$^+$-MS, *m*/*z*: 319.0669 ([Ni(TAP)$_2$ + H]$^+$, requires 319.0670) 567.1173 ([M + H]$^+$, requires 567.1231), 817.1779 ([M + Ni + 2Me$_2$Pz + H]$^+$, requires 817.1763). ν_{max}(KBr)/cm^{-1}: 3376 w, 3368 w ν(N–H); 2994 w, 2944 w, 2918 w, 2856 w ν(C–H); 1614 *vs.* ν(C═N); 1526 s ν(C–N)$_{Pz}$; 1398 s ν(C–O from OMe), 1220 m ν(C–N). ^{1}H NMR ($CDCl_3$, δ): 5.38 (s, 1H, C*H*), 3.78 (s, 6H, OCH_3), 2.46 (s, 6H, C–CH_3). ^{13}C{^{1}H} NMR ($CDCl_3$, δ): 163.8 (*C*═N), 148.0 (*C*H(Pz)), 105.4 (*C*(Pz)), 54.3 (*C*H$_3$O), 13.5 (*C*H$_3$).

[Ni$_2$(μ$_2$-Ph$_2$Pz)$_2$(TAP)$_2$] (3). 71 mg, 34%. Mp: 295 °C (dec.). Anal. calcd for $C_{38}H_{38}N_{10}Ni_2O_4$: C, 55.92; H, 4.69; N, 17.16. Found: C, 55.83; H, 4.67; N, 17.21%. HRESI$^+$-MS, *m*/*z*: 132.0769 ([L + 2H]$^+$, requires 132.0773), *m*/*z*: 319.067 ([Ni(TAP)$_2$ + H]$^+$, requires 319.0665), 628.1979 ([M–Ni–TAP + 2H]$^+$, requires 628.1971), 815.1879 ([M + H]$^+$, requires 815.1863). ν_{max}(KBr)/cm^{-1}: 3372 w, 3340 w ν(N–H); 3064 m, 2990 m, 2940 m, 2858 m ν(C–H); 1618, 1606 *vs.* ν(C═N); 1522 s ν(C–N)$_{Pz}$; 1400 s ν(C–O from OMe), 1232 m ν(C–N). ^{1}H NMR ($CDCl_3$, δ): 8.73 (d, *J* = 7.3 Hz, 4H, CH_{Ar}), 7.60 (t, *J* = 7.0 Hz, 4H, CH_{Ar}), 7.46 (t, *J* = 6.6 Hz, 2H, CH_{Ar}), 6.37 (s, 1H, C*H*), 3.58 (s, 6H, OCH_3). ^{13}C{^{1}H} NMR ($CDCl_3$, δ): 163.4 (*C*═N), 153.4 (*C*H(Pz)), 132.7 (*C*(Ph)), 128.5, 127.8 (*C*H(Ph)), 105.5 (*C*(Pz)), 54.9 (*C*H$_3$O).

[Ni$_3$(μ$_2$-Me$_2$Pz)$_4$(TAP)$_2$] (4). 59 mg, 43%. Mp: 280 °C (dec.). Anal. calcd for $C_{28}H_{44}N_{14}Ni_3O_4$: C, 41.17; H, 5.43; N, 24.01. Found: C, 41.13; H, 5.46; N, 24.04%. HRESI$^+$-MS, *m*/*z*: 132.0755 ([TAP + 2H]$^+$, requires 132.0773), 284.0616 ([Ni(Me$_2$Pz)TAP + H]$^+$, requires 284.0657), 567.1173 ([Ni$_2$(Me$_2$Pz)$_2$(TAP)$_2$ + H]$^+$, requires 567.1231), 817.1663 ([M + H]$^+$, requires 817.1763). ν_{max}(KBr)/cm^{-1}: 3376 w, 3356 w ν(N–H); 2992 w, 2946 w, 2918 w, 2856 w ν(C–H); 1614 *vs.* ν(C═N); 1524 s ν(C–N)$_{Pz}$; 1398 s ν(C–O from OMe), 1222 m ν(C–N). ^{1}H NMR ($CDCl_3$, δ): 5.38 (s, 1H, C*H*), 3.82 (s, 3H, OCH_3), 2.56, 2.22 (two s, 3H, C–CH_3). ^{13}C{^{1}H} NMR ($CDCl_3$, δ): 163.9, 161.5 and 161.1 (*C*═N) and (*C*═O)$_{Me2NCONH2}$, 150.1, 149.9, 149.8, 149.8, 147.3, 147.3, 147.2 (*C*H(Pz)), 106.4, 106.2, 106.2, 106.2, 106.0 (*C*(Pz)), 55.0, 54.4, 53.8 (*C*H$_3$O), 15.3, 14.3, 14.2, 14.0, 13.9, 13.8 (*C*H$_3$).

Conversion of 1 to 2. Complex **1** (16.0 mg, 0.05 mmol) and $NiCl_2$ (6.5 mg, 0.05 mmol) were dissolved in MeOH (5 mL) at RT, whereupon HMe_2Pz (39.5 mg, 0.4 mmol) was added. The homogeneous yellowish-brown reaction mixture was left to stand at 50 °C in a closed flask. After 30 min the color of the reaction mixture gradually turned to yellow and the yellow precipitate was released. The reaction mixture was left to stand at 50 °C for 1 d in a closed flask. The mother liquor was decanted, the product was washed with three 1.5 mL portions of MeOH and with three 1.5 mL portions of Et_2O. The crystalline product dried over $CaCl_2$ in a desiccator at 20–25 °C. The yield of **2** is 5.3 mg, 19%. HRESI$^+$-MS for the mother liquor, *m*/*z*: 284.0638 ([Ni(Me$_2$Pz)TAP + H]$^+$, requires 284.0657), 319.0650 ([Ni(TAP)$_2$ + H]$^+$ requires 319.0670), 380.1343 ([M–Ni–TAP + 2H]$^+$, requires 284.1345), 567.1190 ([M + H]$^+$, requires 567.1231). Complex **2** was also identified using powder XRD (Fig. S26, ESI†).

Conversion of 1 to 3. (R′ = Ph) was conducted similarly. The system comprised of [Ni(TAP)$_2$] (**1**) (9.0 mg, 0.03 mmol), $NiCl_2$ (4.1 mg, 0.03 mmol), MeOH (1.5 mL), and HPh_2Pz (54.2 mg, 0.25 mmol) was used. The yield of **3** is 3.3 mg, 14%. Mother liquor: HRESI$^+$, *m*/*z*: 221.1087 ([HPh$_2$Pz + H]$^+$, requires 221.1079), 319.0686 ([Ni(TAP)$_2$ + H]$^+$, requires 319.0670), 628.2004 ([M–Ni–TAP + 2H]$^+$, requires 628.1971). A solution of **3** in $CHCl_3$. HRESI$^+$, *m*/*z*: 221.1085 ([HPh$_2$Pz + H]$^+$, requires 221.1079), 319.0681 ([Ni(TAP)$_2$ + H]$^+$, requires 319.0670), 628.1993 ([M–Ni–TAP + 2H]$^+$, requires 628.1971), 815.1865 ([M + H]$^+$, requires 815.1863).

Conversion of 1 to 5. Complex **1** (3.0 mg, 0.0094 mmol) and $NiCl_2$ (1.3 mg, 0.010 mmol) were dissolved in MeOH (2 mL) at RT, whereupon HInd (7.1 mg, 0.060 mmol) was added. The homogeneous pale rose reaction mixture was left to stand at 50 °C in a closed flask. After 30 min the color of the reaction mixture gradually turned to pale yellow. The solution was left to stand at 50 °C for 7 d in a closed flask, whereupon the solvent slowly evaporated at RT. Reaction solution: HRESI$^+$, *m*/*z*: 319.0671

($[Ni(TAP)_2 + H]^+$ requires 319.0670), 611.0918 ($[Ni_2(\mu_2\text{-Ind})_2(TAP)_2 + H]^+$ requires 611.0924), 905.1054 ($[Ni_3(\mu_2\text{-Ind})_4(TAP)_2 + H]^+$ requires 905.1137).

Conversion of 2 to 4. $[Ni_2(\mu_2\text{-}Me_2Pz)_2(TAP)_2]$ (8.3 mg, 0.015 mmol) and $NiCl_2$ (1.9 mg, 0.015 mmol) were dissolved at RT in a mixture of DMF (1.5 mL) and $NCNMe_2$ (3.2 mg, 0.046 mmol), whereupon HMe_2Pz (18.4 mg, 0.19 mmol) was added. The homogeneous yellow reaction mixture formed was left to stand at 110 °C in a closed flask. After 1 d the yellow-orange precipitate released, was decanted, washed with three 1.5 mL portions of MeOH and with three 1.5 mL portions of Et_2O. The crystalline product dried over $CaCl_2$ in a desiccator at 20–25 °C. The yield of **4** is 6.4 mg, 52% based on Ni. HRESI$^+$ (mother liquor), *m*/*z*: 567.1253 ($[Ni_2(Me_2Pz)_2(TAP)_2 + H]^+$, requires 567.1231), 817.1793 ($[M + H]^+$, requires 817.1763). The crystalline phase of $[Ni_3(\mu_2\text{-}Me_2Pz)_4(TAP)_2]$ was identified by powder XRD (Fig. S27, ESI†).

Conversion of 2 to 1. Complex **2** (14.2 mg, 0.025 mmol) was dissolved in $CHCl_3$ (1 mL) at RT, whereupon glacial acetic acid (1.2 mg, 0.02 mmol) was added to the solution. The bright yellow homogeneous solution formed was left to stand at 50 °C in a closed flask. After 2 d the color of the reaction mixture turned to pale yellow and a pale blue amorphous precipitate was released, which was centrifuged and the mother liquor was evaporated at RT to dryness. Pink crystals were grown from the mother liquor. The yield of **1** is 1.5 mg, 19% based on Ni. HRESI$^+$, *m*/*z*: 319.0669 ($[M + H]^+$, requires 319.0670).

Conversion of 4 to 1. This conversion was conducted similarly to the previous method. Complex **4** (11.3 mg, 0.014 mmol) and glacial acetic acid (0.8 mg, 0.013 mmol) were used. The yield of **1** is 1.0 mg, 22% based on Ni. HRESI$^+$, *m*/*z*: 319.0676 ($[M + H]^+$, requires 319.0670).

Acknowledgements

The synthetic part of this combined project was supported by the Russian Science Foundation (grant 14-13-00060), whereas the theoretical part was conducted under the Russian Foundation for Basic Research project (grant 16-33-60063). The authors thank the Center for X-ray Diffraction Studies, the Center for Magnetic Resonance, the Center for Thermogravimetric and Calorimetric Research, the Center for Chemical Analysis and Materials Research, the Chemistry Educational Center, and "Geomodel" (which all belong to Saint Petersburg State University) for the physicochemical measurements.

References

1 (*a*) S. Trofimenko, *Scorpionates: The Coordination Chemistry of Polypyrazolylborate Ligands*, Imperial College Press, London, 1999; (*b*) S. Trofimenko, *J. Chem. Educ.*, 2005, **82**, 1715–1720.
2 C. Pettinari, A. Tabacaru and S. Galli, *Coord. Chem. Rev.*, 2016, **307**, 1–31.
3 (*a*) E. D. Doidge, J. W. Roebuck, M. R. Healy and P. A. Tasker, *Coord. Chem. Rev.*, 2015, **288**, 98–117; (*b*) M. Viciano-Chumillas, S. Tanase, L. J. de Jongh and J. Reedijk, *Eur. J. Inorg. Chem.*, 2010, 3403–3418, DOI: 10.1002/ejic.201000412; (*c*) I. Castro, W. P. Barros, M. L. Calatayud, F. Lloret, N. Marino, G. De Munno, H. O. Stumpf, R. Ruiz-García and M. Julve, *Coord. Chem. Rev.*, 2016, **315**, 135–152; (*d*) W. P. Barros, M. Luisa Calatayud, F. Lloret, M. Julve, N. Marino, G. De Munno, H. O. Stumpf, R. Ruiz-Garcia and I. Castro, *CrystEngComm*, 2016, **18**, 437–449; (*e*) J.-Y. Xu, X. Qiao, H.-B. Song, S.-P. Yan, D.-Z. Liao, S. Gao, Y. Journaux and J. Cano, *Chem. Commun.*, 2008, 6414–6416, DOI: 10.1039/B813705F.
4 (*a*) M. A. Halcrow, *Dalton Trans.*, 2009, 2059–2073, DOI: 10.1039/b815577a; (*b*) J. Perez and L. Riera, *Eur. J. Inorg. Chem.*, 2009, 4913–4925, DOI: 10.1002/ejic.200900694; (*c*) L. Hou, W.-J. Shi, Y.-Y. Wang, H.-H. Wang, L. Cui, P.-X. Chen and Q.-Z. Shi, *Inorg. Chem.*, 2011, **50**, 261–270; (*d*) L.-Y. Du, W.-J. Shi, L. Hou, Y.-Y. Wang, Q.-Z. Shi and Z. Zhu, *Inorg. Chem.*, 2013, **52**, 14018–14027.
5 K. E. Dalle and F. Meyer, *Eur. J. Inorg. Chem.*, 2015, 3391–3405, DOI: 10.1002/ejic.201500185.
6 (*a*) J. Tong, S.-Y. Yu and H. Li, *Chem. Commun.*, 2012, **48**, 5343–5345; (*b*) G.-H. Ning, L.-Y. Yao, L.-X. Liu, T.-Z. Xie, Y.-Z. Li, Y. Qin, Y.-J. Pan and S.-Y. Yu, *Inorg. Chem.*, 2010, **49**, 7783–7792.
7 N. Masciocchi, G. A. Ardizzoia, S. Brenna, G. LaMonica, A. Maspero, S. Galli and A. Sironi, *Inorg. Chem.*, 2002, **41**, 6080–6089.
8 C. J. Adams, M. A. Kurawa and A. G. Orpen, *Dalton Trans.*, 2010, **39**, 6974–6984.
9 (*a*) S. Galli, N. Masciocchi, V. Colombo, A. Maspero, G. Palmisano, F. J. Lopez-Garzon, M. Domingo-Garcia, I. Fernandez-Morales, E. Barea and J. A. R. Navarro, *Chem. Mater.*, 2010, **22**, 1664–1672; (*b*) E. Albanese, B. Civalleri, M. Ferrabone, F. Bonino, S. Galli, A. Maspero and C. Pettinari, *J. Mater. Chem.*, 2012, **22**, 22592–22602.
10 K. S. M. Salih, S. Bergner, H. Kelm, Y. Sun, A. Grün, Y. Schmitt, R. Schoch, M. Busch, N. Deibel, S. Bräse, B. Sarkar, M. Bauer, M. Gerhards and W. R. Thiel, *Eur. J. Inorg. Chem.*, 2013, 6049–6059.
11 (*a*) W. Tan, Z. Yu, B. Liu, K. Wu, Z. Liu and J. Chen, *J. Organomet. Chem.*, 2009, **694**, 199–206; (*b*) S. J. Rettig, A. Storr, D. A. Summers, R. C. Thompson and J. Trotter, *Can. J. Chem.*, 1997, **75**, 949–958.
12 K. Fujita, S. Hikichi, M. Akita and Y. Moro-oka, *J. Chem. Soc., Dalton Trans.*, 2000, 117–119, DOI: 10.1039/A908181J.
13 S. Mukhopadhyay, U. Mukhopadhyay, T. C. W. Mak and D. Ray, *Inorg. Chem.*, 2001, **40**, 1057–1059.
14 P. Espinet, A. M. Gallego, J. M. Martínez-Ilarduya and E. Pastor, *Inorg. Chem.*, 2000, **39**, 975–979.
15 S.-J. Jeon and R. M. Waymouth, *Dalton Trans.*, 2008, 437–439, DOI: 10.1039/B715212D.
16 Y. Zhou, Z. Xi, W. Chen and D. Wang, *Organometallics*, 2008, **27**, 5911–5920.
17 (*a*) P. J. Altmann, C. Jandl and A. Pothig, *Dalton Trans.*, 2015, **44**, 11278–11281; (*b*) P. J. Altmann and A. Pöthig, *Chem. Commun.*, 2016, **52**, 9089–9092, DOI: 10.1039/C6CC00507A.
18 E. Quartapelle Procopio, S. Rojas, N. M. Padial, S. Galli, N. Masciocchi, F. Linares, D. Miguel, J. E. Oltra,

J. A. R. Navarro and E. Barea, *Chem. Commun.*, 2011, **47**, 11751–11753.

19 J.-Y. Xu, H.-B. Song, G.-F. Xu, X. Qiao, S.-P. Yan, D.-Z. Liao, Y. Journaux and J. Cano, *Chem. Commun.*, 2012, **48**, 1015–1017.

20 (*a*) N. A. Bokach, *Russ. Chem. Rev.*, 2010, **79**, 89–100; (*b*) N. A. Bokach, M. L. Kuznetsov and V. Y. Kukushkin, *Coord. Chem. Rev.*, 2011, **255**, 2946–2967; (*c*) N. A. Bokach and V. Y. Kukushkin, *Russ. Chem. Rev.*, 2005, **74**, 153–170; (*d*) N. A. Bokach and V. Y. Kukushkin, *Coord. Chem. Rev.*, 2013, **257**, 2293–2316; (*e*) V. Y. Kukushkin and A. J. L. Pombeiro, *Chem. Rev.*, 2002, **102**, 1771–1802; (*f*) V. Y. Kukushkin and A. J. L. Pombeiro, *Inorg. Chim. Acta*, 2005, **358**, 1–21; (*g*) A. J. L. Pombeiro and V. Y. Kukushkin, *Compr. Coord. Chem. II*, 2004, **1**, 639–660.

21 (*a*) A. V. Khripun, V. Y. Kukushkin, S. I. Selivanov, M. Haukka and A. J. L. Pombeiro, *Inorg. Chem.*, 2006, **45**, 5073–5083; (*b*) M. A. Kinzhalov, K. V. Luzyanin, V. P. Boyarskiy, M. Haukka and V. Y. Kukushkin, *Russ. Chem. Bull.*, 2013, **62**, 758–766.

22 (*a*) R. Boca, M. Hvastijova and J. Kozisek, *J. Chem. Soc., Dalton Trans.*, 1995, 1921–1923; (*b*) G. Goetz and H. U. Kibbel, *Z. Chem.*, 1975, **15**, 278–280.

23 (*a*) I. M. Atkinson, M. M. Bishop, L. F. Lindoy, S. Mahadev and P. Turner, *Chem. Commun.*, 2002, 2818–2819, DOI: 10.1039/b206898b; (*b*) M. M. Bishop, L. F. Lindoy, S. Mahadev and P. Turner, *J. Chem. Soc., Dalton Trans.*, 2000, 233–234; (*c*) M. N. Kopylovich, Y. Y. Karabach, M. F. C. Guedes da Silva, P. J. Figiel, J. Lasri and A. J. L. Pombeiro, *Chem. – Eur. J.*, 2012, **18**, 899–914; (*d*) L.-L. Zheng, J.-D. Leng, W.-T. Liu, W.-X. Zhang, J.-X. Lu and M.-L. Tong, *Eur. J. Inorg. Chem.*, 2008, 4616–4624, DOI: 10.1002/ejic.200800486; (*e*) M.-L. Tong, Y.-M. Wu, Y.-X. Tong, X.-M. Chen, H.-C. Chang and S. Kitagawa, *Eur. J. Inorg. Chem.*, 2003, 2385–2388.

24 G. Rembarz, E. Fischer, K. C. Roeber, R. Ohff and H. Crahmer, *J. Prakt. Chem.*, 1969, **311**, 889–892.

25 M. N. Kopylovich, J. Lasri, M. F. C. Guedes da Silva and A. J. L. Pombeiro, *Eur. J. Inorg. Chem.*, 2011, 377–383, DOI: 10.1002/ejic.201000898.

26 S. Alvarez, *Dalton Trans.*, 2013, **42**, 8617–8636.

27 R. F. W. Bader, *Atoms in Molecules: A Quantum Theory*, Oxford University Press, Oxford, 1990.

28 (*a*) X. Ding, M. J. Tuikka, P. Hirva, V. Y. Kukushkin, A. S. Novikov and M. Haukka, *CrystEngComm*, 2016, **18**, 1987–1995; (*b*) A. S. Novikov, M. L. Kuznetsov and A. J. L. Pombeiro, *Chem. – Eur. J.*, 2013, **19**, 2874–2888; (*c*) D. M. Ivanov, A. S. Novikov, I. V. Ananyev, Y. V. Kirina and V. Y. Kukushkin, *Chem. Commun.*, 2016, **52**, 5565–5568; (*d*) T. V. Serebryanskaya, A. S. Novikov, P. V. Gushchin, M. Haukka, R. E. Asfin, P. Tolstoy and V. Y. Kukushkin, *Phys. Chem. Chem. Phys.*, 2016, **18**, 14104–14112; (*e*) V. N. Mikhaylov, V. N. Sorokoumov, K. A. Korvinson, A. S. Novikov and I. A. Balova, *Organometallics*, 2016, **35**, 1684–1697; (*f*) D. M. Ivanov, A. S. Novikov, G. L. Starova, M. Haukka and V. Y. Kukushkin, *CrystEngComm*, 2016, **18**, 5278–5286.

29 (*a*) V. W. Yam and K. K. Lo, *Chem. Soc. Rev.*, 1999, **28**, 323–334; (*b*) N. L. Coker, J. A. Krause Bauer and R. C. Elder, *J. Am. Chem. Soc.*, 2004, 12–13; (*c*) B. Liu, W. Chen and S. Jin, *Organometallics*, 2007, **26**, 3660–3667.

30 V. W.-W. Yam, K. M.-C. Wong and N. Zhu, *J. Am. Chem. Soc.*, 2002, **124**, 6506–6507.

31 D. B. Leznoff, B.-Y. Xue, C. L. Stevens, A. Storr, R. C. Thompson and B. O. Patrick, *Polyhedron*, 2001, **20**, 1247–1254.

32 (*a*) S. Myllynen and M. Wasberg, *Electrochem. Commun.*, 2009, **11**, 1453–1456; (*b*) M. Mitsumi, H. Ueda, K. Furukawa, Y. Ozawa, K. Toriumi and M. Kurmoo, *J. Am. Chem. Soc.*, 2008, **130**, 14102–14104; (*c*) M. Mitsumi, H. Goto, S. Umebayashi, Y. Ozawa, M. Kobayashi, T. Yokoyama, H. Tanaka, T. Kuroda and K. Toriumi, *Angew. Chem., Int. Ed.*, 2005, **44**, 4164–4168.

33 W. B. Connick, R. E. Marsh, W. P. Schaefer and H. B. Gray, *Inorg. Chem.*, 1997, **36**, 913–922.

34 A. Orthaber, S. Borucki, W. Shen, R. Réau, C. Lescop and R. Pietschnig, *Eur. J. Inorg. Chem.*, 2014, 1751–1759.

35 S. Sculfort and P. Braunstein, *Chem. Soc. Rev.*, 2011, **40**, 2741–2760.

36 (*a*) M. R. R. Prabhath, J. Romanova, R. J. Curry, S. R. P. Silva and P. D. Jarowski, *Angew. Chem., Int. Ed.*, 2015, **54**, 7949–7953; (*b*) A. Aliprandi, D. Genovese, M. Mauro and L. De Cola, *Chem. Lett.*, 2015, **44**, 1152–1169; (*c*) V. V. Sivchik, E. V. Grachova, A. S. Melnikov, S. N. Smirnov, A. Y. Ivanov, P. Hirva, S. P. Tunik and I. O. Koshevoy, *Inorg. Chem.*, 2016, **55**, 3351–3363; (*d*) B.-H. Xia, C.-M. Che, D. L. Phillips, K.-H. Leung and K.-K. Cheung, *Inorg. Chem.*, 2002, **41**, 3866–3875; (*e*) B.-H. Xia, C.-M. Che and Z.-Y. Zhou, *Chem. – Eur. J.*, 2003, **9**, 3055–3064; (*f*) H.-K. Yip, T.-F. Lai and C.-M. Che, J. Chem. Soc., *Dalton Trans.*, 1991, 1639–1641; (*g*) I. M. Sluch, A. J. Miranda, O. Elbjeirami, M. A. Omary and L. M. Slaughter, *Inorg. Chem.*, 2012, **51**, 10728–10746.

37 (*a*) M. Weber, J. E. M. N. Klein, B. Miehlich, W. Frey and R. Peters, *Organometallics*, 2013, **32**, 5810–5817; (*b*) D. L. J. Broere, S. Demeshko, B. de Bruin, E. A. Pidko, J. N. H. Reek, M. A. Siegler, M. Lutz and J. I. van der Vlugt, *Chem. – Eur. J.*, 2015, **21**, 5879–5886; (*c*) A. Gouranourimi, M. Ghassemzadeh and S. Bahemmat, *Monatsh. Chem.*, 2015, **146**, 57–67.

38 (*a*) M. Himmelsbach, R. L. Lintvedt, J. K. Zehetmair, M. Nanny and M. J. Heeg, *J. Am. Chem. Soc.*, 1987, **109**, 8003–8011; (*b*) S. J. R. Kenneth, S. Chong, A. Storr and J. Trotter, *Can. J. Chem.*, 1981, **59**, 996–1006; (*c*) B. Ding, L. Yi, W.-Z. Shen, P. Cheng, D.-Z. Liao, S.-P. Yan and Z.-H. Jiang, *J. Mol. Struct.*, 2006, 138–143, DOI: 10.1016/j.molstruc.2005.08.025; (*d*) M. Maekawa, M. Munakata, T. Kuroda and Y. Nozaka, *Inorg. Chim. Acta*, 1993, **208**, 243–244.

39 E. Espinosa, E. Molins and C. Lecomte, *Chem. Phys. Lett.*, 1998, **285**, 170–173.

40 M. V. Vener, A. N. Egorova, A. V. Churakov and V. G. Tsirelson, *J. Comput. Chem.*, 2012, **33**, 2303–2309.

41 (*a*) J. Lai, W. Niu, R. Luque and G. Xu, *Nano Today*, 2015, **10**, 240–267; (*b*) Y. Zhao, K. Li and J. Li, *Z. Naturforsch.*, 2010, 976–998.

42 A. R. Pray, R. F. Heitmiller, S. Strycker, V. D. Aftandilian, T. Muniyappan, D. Choudhury and M. Tamres, *Inorg. Synth.*, 2007, **28**, 321.

43 D. Harvey, *Modern analytical chemistry*, McGraw-Hill Companies Inc., International ed, 2000.

44 *NETZSCH Proteus Software v.6.1.*, Netzsch-Gerätebau, Bayern, Germany, 2013.
45 G. M. Sheldrick, *Acta Crystallogr.*, 2008, **A64**, 112.
46 (*a*) L. Palatinus and G. Chapuis, *J. Appl. Crystallogr.*, 2007, **40**, 786–790; (*b*) L. Palatinus and A. van der Lee, *J. Appl. Crystallogr.*, 2008, **41**, 975–984; (*c*) L. Palatinus, S. J. Prathapa and S. van Smaalen, *J. Appl. Crystallogr.*, 2012, **45**, 575–580.
47 O. V. Dolomanov, L. J. Bourhis, R. J. Gildea, J. A. K. Howard and H. Puschmann, *J. Appl. Crystallogr.*, 2009, **42**, 339–341.
48 A. L. Spek, *PLATON, A Multipurpose Crystallographic Tool*, Utrecht University, Utrecht, The Netherlands, 2005.
49 Y. Zhao and D. G. Truhlar, *Theor. Chem. Acc.*, 2008, **120**, 215–241.
50 M. J. Frisch, G. W. Trucks, H. B. Schlegel, G. E. Scuseria, M. A. Robb, J. R. Cheeseman, G. Scalmani, V. Barone, B. Mennucci, G. A. Petersson, H. Nakatsuji, M. Caricato, X. Li, H. P. Hratchian, A. F. Izmaylov, J. Bloino, G. Zheng, J. L. Sonnenberg, M. Hada, M. Ehara, K. Toyota, R. Fukuda, J. Hasegawa, M. Ishida, T. Nakajima, Y. Honda, O. Kitao, H. Nakai, T. Vreven, J. A. Montgomery Jr., J. E. Peralta, F. Ogliaro, M. Bearpark, J. J. Heyd, E. Brothers, K. N. Kudin, V. N. Staroverov, T. Keith, R. Kobayashi, J. Normand, K. Raghavachari, A. Rendell, J. C. Burant, S. S. Iyengar, J. Tomasi, M. Cossi, N. Rega, J. M. Millam, M. Klene, J. E. Knox, J. B. Cross, V. Bakken, C. Adamo, J. Jaramillo, R. Gomperts, R. E. Stratmann, O. Yazyev, A. J. Austin, R. Cammi, C. Pomelli, J. W. Ochterski, R. L. Martin, K. Morokuma, V. G. Zakrzewski, G. A. Voth, P. Salvador, J. J. Dannenberg, S. Dapprich, A. D. Daniels, O. Farkas, J. B. Foresman, J. V. Ortiz, J. Cioslowski and D. J. Fox, *Gaussian 09, Revision C.01*, Gaussian, Inc., Wallingford, CT, 2010.
51 M. Reiher, *Wiley Interdiscip. Rev.: Comput. Mol. Sci.*, 2012, **2**, 139–149.
52 (*a*) F. E. Jorge, A. Canal Neto, i. G. G. Camilett and S. F. Machado, *J. Chem. Phys.*, 2009, **130**, 064108; (*b*) A. Canal Neto and F. E. Jorge, *Chem. Phys. Lett.*, 2013, **582**, 158–162; (*c*) R. C. de Berredo and F. E. Jorge, *THEOCHEM*, 2010, **961**, 107–112; (*d*) C. L. Barros, P. J. P. de Oliveira, F. E. Jorge, A. C. Neto and M. Campos, *Mol. Phys.*, 2010, **108**, 1965–1972.
53 T. Lu and F. W. Chen, *J. Comput. Chem.*, 2012, **33**, 580–592.